Available online at www.sciencedirect.com
ScienceDirect
Journal of Nuclear Materials 358 (2006) 202–208
journal of nuclear materials
www.elsevier.com/locate/jnucmat

Effects of HCO_3^- on the kinetics of UO_2 oxidation by H_2O_2

Mohammad Mohsin Hossain, Ella Ekeroth, Mats Jonsson *

Department of Chemistry, Nuclear Chemistry, Royal Institute of Technology, SE-100 44 Stockholm, Sweden

Received 5 December 2005; accepted 17 July 2006

Abstract

The effect of HCO_3^- on the kinetics of UO_2 oxidation by H_2O_2 in aqueous solution has been studied using powder suspensions where the concentration of H_2O_2 was monitored as a function of time. By varying the UO_2 surface to solution volume ratio second order rate constants were obtained for HCO_3^- concentrations ranging from 0 to 100 mM. The second order rate constant increases linearly with HCO_3^- concentration from 0 to approximately 1 mM. Above 1 mM HCO_3^- the rate constant is 4.4×10^{-6} m min^{-1} independent of $[HCO_3^-]$. This indicates that the kinetics of the reaction depends on both oxidation and dissolution below 1 mM HCO_3^- while at higher concentrations it is solely governed by oxidation. Hence, the rate constant obtained at HCO_3^- concentrations above 1 mM is the true rate constant for oxidation of UO_2 by H_2O_2. The results also imply that the reaction between HCO_3^- and oxidized UO_2 on the UO_2 surface (i.e. HCO_3^- facilitated dissolution) is limited by diffusion (ca 10^{-3} m min^{-1} in the present system). Furthermore, the experimental results were used to estimate the oxidation site density of the powder used (126 sites nm^{-1}) and the rate constant for dissolution of UO_2^{2+} from the UO_2 surface (7×10^{-8} mol m^{-2} s^{-1}).

1. Introduction

The possible release of toxic and radioactive species from spent nuclear fuel in contact with water in a future deep repository is expected to depend mainly on the rate of dissolution of the UO_2 matrix [1]. In the reducing groundwater expected at the depth of a repository, UO_2 has very low solubility [2]. However, radiolysis of the ground water will produce reactive radicals and molecular products (e_{aq}^-, H$^\cdot$, H_2 (reductants) and OH$^\cdot$, H_2O_2 (oxidants)) [3] and thereby alter the reducing environment. Secondary reactions will produce $HO_2^\cdot$, $O_2^{\cdot-}$ and O_2 and with carbonate present in the ground water, $CO_3^{\cdot-}$ will be produced. OH$^\cdot$ and $CO_3^{\cdot-}$ are both strong one-electron oxidants ($E^0 = 1.9$ V and 1.59 V vs. NHE, respectively [4,5]) while $HO_2^\cdot$ and $O_2^{\cdot-}$ are fairly weak one-electron oxidants (depending on pH). H_2O_2 and O_2 on the other hand can act both as one- and two-electron oxidants.

The presence of carbonate affects the kinetics for UO_2 oxidation not only by converting OH$^\cdot$ into $CO_3^{\cdot-}$ but also since it forms soluble complexes with the oxidation product, UO_2^{2+} [6], and thereby maintains a larger surface area accessible to oxidation.

In a previous paper we studied the kinetics for oxidation of UO_2 in aqueous solution by various

* Corresponding author. Tel.: +46 8 7909123; fax: +46 8 7908772.
E-mail address: matsj@nuchem.kth.se (M. Jonsson).

0022-3115/$ - see front matter © 2006 Elsevier B.V. All rights reserved.
doi:10.1016/j.jnucmat.2006.07.008

oxidants [7]. From experimental data we were able to establish a linear relationship between the logarithm of the rate constant and the one-electron reduction potential of the oxidant. Both one- and two-electron oxidants were found to follow this relationship and it was therefore concluded that the first one-electron transfer is the rate determining step also for two-electron oxidants. This implies that oxidation of UO_2 by H_2O_2 is a Fenton-like two step process:

$$UO_2 + H_2O_2 \rightarrow UO_2^+ + OH^{\cdot} + OH^- \quad (1)$$

$$OH^{\cdot} + UO_2^+ \rightarrow OH^- + UO_2^{2+} \quad (2)$$

where $k_2 \gg k_1$. On the basis of the established relationship and simple collision theory [8], the strongest oxidants expected to occur during radiolysis ($OH^{\cdot}$ and $CO_3^{\cdot -}$) of groundwater would have rate constants limited by diffusion. Hence, both radicals are expected to be equally reactive towards UO_2. It should, however, be noted that the impact of the two radicals on UO_2 dissolution may differ considerably due to differences in reactivity towards other species present in the system affecting the life-time of the radicals.

The kinetic studies in Ref. [7] were performed in carbonate free solutions and the reported rate constants are, therefore, probably significantly affected by the dissolution of oxidized UO_2 and, hence, are not the accurate rate constants for oxidation. The effect of HCO_3^- on the kinetics for UO_2 oxidation by H_2O_2 was also investigated qualitatively in Ref. [7]. It was clearly shown that the rate of UO_2 dissolution as well as of UO_2 oxidation (consumption of H_2O_2) increased with increasing carbonate concentration. This has also been shown previously by other authors [9–12]. The presence of carbonate has also been suggested to reduce the efficiency of the oxidant (H_2O_2) due to the conversion of $OH^{\cdot}$ into $CO_3^{\cdot -}$ where the latter was claimed to be less reactive towards UO_2 [11]. However, judging from our previous work, this does not seem to be a plausible explanation. It should be noted that, in aqueous solutions containing H_2O_2 and HCO_3^-, peroxymonocarbonate (HCO_4^-) can be formed [13]. The reactivity of peroxymonocarbonate towards UO_2 is not known, but judging from the reported redox properties it should be similar to that of H_2O_2 [14]. In this work we have performed a quantitative study of the effect of HCO_3^- concentration on the second order rate constant for the reaction between H_2O_2 and UO_2 in aqueous UO_2-particle suspensions. This was done by determining the second order rate constant at eight different HCO_3^- concentrations ranging from 0 to 100 mM.

2. Experimental

The UO_2 powder was supplied from Westinghouse Atom AB. Chemicals and gases used were of purest grade available and were obtained from Lancaster, Perstorp AB, Merck, Alfa, BDH and AGA. Millipore Milli-Q filtered water was used throughout. The UO_2 powder used in this work has a specific area of 5.85 m^2/g given by BET measurements (He/N_2, 70/30). When studying the effect of carbonate on the reaction between H_2O_2 and UO_2, the UO_2 powder was washed three times with $NaHCO_3$ solutions of the same concentration as in the subsequent experiments.

The suspensions (18 ml) initially containing 18 mM H_2O_2, 50–200 mg UO_2 and 0–100 mM HCO_3^- were purged with Argon throughout the experiments and stirred by a magnetic stirrer. For each HCO_3^- concentration, experiments using 4–5 different amounts of UO_2 were performed in order to allow for determination of the second order rate constant. The sample volume taken for analysis was approximately 2 ml. Before analysis, the solution was filtered (pore size 0.20 μm) to stop the reaction and to clear the solution.

The concentration of H_2O_2 was measured indirectly by UV/visible spectroscopy (Jasco V-530 UV/VIS-Spectrophotometer). The H_2O_2 solutions were protected from light during the experiments. We have used I_3^- as 'indicator' for analysis of the hydrogen peroxide concentration at 360 nm where I_3^- absorbs (reactions (3) and (4)):

$$H_2O_2 + 2H^+ + 2I^- \rightarrow 2H_2O + I_2 \quad (3)$$

$$I_2 + I^- \rightarrow I_3^- \quad (4)$$

The sample was mixed with 100 μl potassium iodide (1 M KI) and 100 μl acetate buffer which contained ammonium molybdate (catalyst) (1 M HAc/NaAc, a few drops of 3% $(NH_4)_2Mo_2O_7$ (ADM) to 100 ml solution) and water to a total volume of 2 ml. Using this method, μM concentrations of H_2O_2 are detectable. Detailed information about the I_3^- method can be found in Refs. [15–17].

3. Results and discussion

In the kinetic studies the UO_2 surface is assumed to be in excess compared to the oxidants. Hence, the reactions can at least initially be treated as being pseudo-first order. In Fig. 1 the concentration of H_2O_2 in suspensions containing 50 mg UO_2 is given as a function of time at different concentrations of HCO_3^-.

As can be seen, the rate of H_2O_2 consumption in the system increases significantly with increasing HCO_3^- concentration.

In Fig. 2 the concentration of H_2O_2 in suspensions containing various amounts of UO_2 and 100 mM HCO_3^- is given as a function of time.

As expected, the rate of H_2O_2 consumption increases with increasing amount of UO_2 (increasing surface to volume ratio). It is interesting to note that, when plotting the concentration of H_2O_2 versus time, for experiments performed at low carbonate concentrations the reaction is initially of first order but in a relatively short time becomes a reaction of zeroth order, i.e. the reaction rate becomes independent of H_2O_2 concentration. The change in reaction order occurs at different H_2O_2 conversions depending both on the amount of UO_2 and the concentration of HCO_3^-. The reason for this behaviour is probably that a significant fraction of the UO_2 surface becomes covered by oxidation products and, in the absence HCO_3^- ($[H_2O_2]$ is more than a factor 20 higher than $[HCO_3^-]$ in the experiments where zeroth order behaviour is observed), the rate limiting step becomes dissolution of UO_2^{2+} rather than oxidation of UO_2. The implications of this will be discussed in more detail later on.

The second order rate constant can be obtained from the slope in a plot where the pseudo-first order rate constant, $k\,(\mathrm{min}^{-1})$ (obtained by plotting $\ln[H_2O_2]$ against reaction time) is plotted against the solid surface/total solution volume ratio, S/V (m^{-1}). An example is given in Fig. 3. It should, however, be stressed that the analysis of the pseudo-first order reactions should only be based on the initial part of the plot ($\ln[H_2O_2]$ vs time) where first order behavior is observed. The resulting second order rate constants for all HCO_3^- concentrations studied in this work are presented in Table 1.

As can be seen in Table 1 the second order rate constant increases by a factor of two between the lowest and the highest HCO_3^- concentrations. The HCO_3^- concentration dependence is illustrated in Fig. 4 for the concentration range 0–1 mM.

From Table 1 and Fig. 4 we can make two important observations: (1) The second order rate constant for the reaction increases linearly with HCO_3^- concentration in the 0–1 mM concentration range. (2) The second order rate constant is independent of HCO_3^- concentration above 1 mM. Before discussing the results further we must introduce the following general reaction mechanism including oxidation (reaction (5)) and HCO_3^- facilitated dissolution of the oxidation product (reaction (6)):

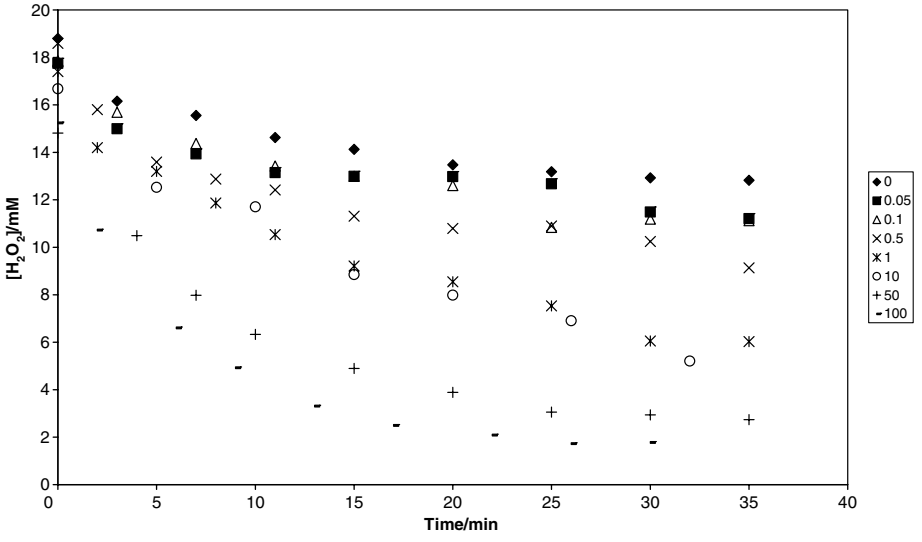

Fig. 1. Concentration of H_2O_2 in suspensions containing 50 mg UO_2 as a function of time at different concentrations of HCO_3^- (mM).

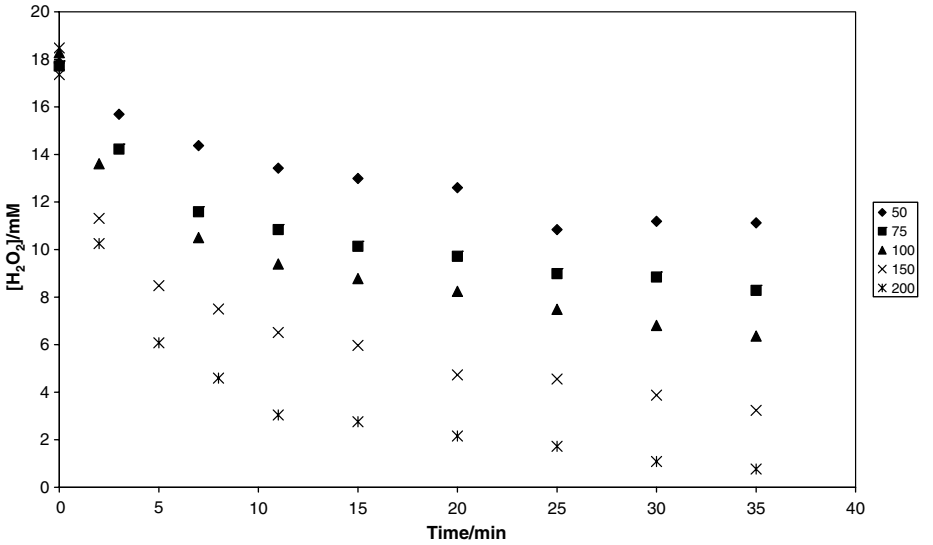

Fig. 2. Concentration of H_2O_2 in suspensions containing various amounts of UO_2 (mg) and 100 mM HCO_3^- as a function of time.

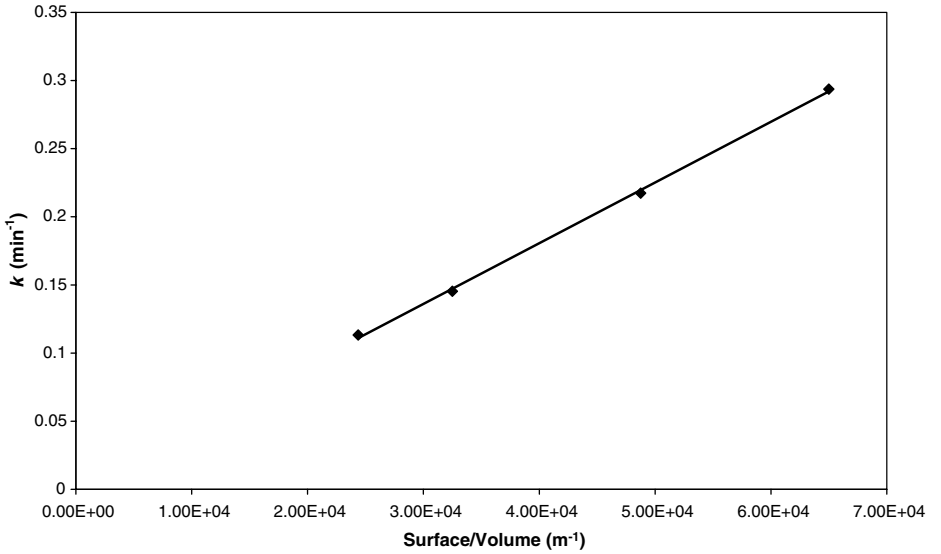

Fig. 3. The pseudo-first order rate constant, $k\,(\mathrm{min}^{-1})$ plotted against the solid surface/total solution volume ratio, S/V (m^{-1}). $[HCO_3^-] = 100$ mM.

Table 1
Second order rate constant for the reaction between H_2O_2 and UO_2 at different concentrations of added HCO_3^-

Added $[HCO_3^-]$ (mM)	k $(\mathrm{m\,min}^{-1})$
0	1.9×10^{-6}
0.05	1.9×10^{-6}
0.1	2.1×10^{-6}
0.5	3.2×10^{-6}
1	4.6×10^{-6}
10	4.0×10^{-6}
50	4.6×10^{-6}
100	4.5×10^{-6}

$$(UO_2)_{n(s)} + H_2O_2 \rightarrow (UO_2)_{n-1}UO_{2(s)}^{2+} + 2OH^- \quad (5)$$

$$(UO_2)_{n-1}UO_{2(s)}^{2+} + xHCO_3^- \rightarrow UO_2(CO_3)_x^{(2-2x)}(aq) + xH^+ + (UO_2)_{n-1(s)} \quad (6)$$

Reaction (5) represents the combined effect of reactions (1) and (2). Since reaction (1) is rate determining we can, from a kinetic point of view, combine the two consecutive one-electron transfer processes into a single two-electron transfer step.

Judging from Fig. 4 and Table 1, the observed reaction rate depends on both reactions (5) and (6)

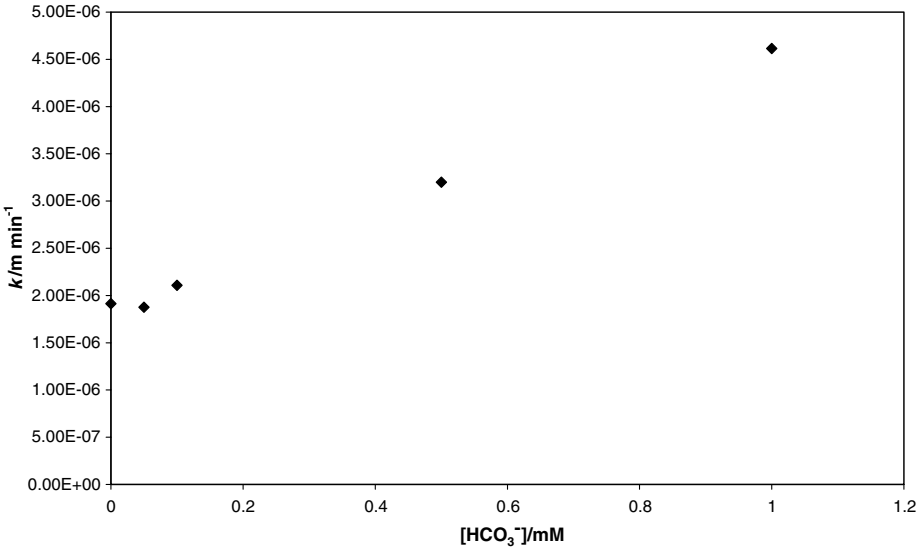

Fig. 4. The second order rate constant for oxidation of UO_2 by H_2O_2 as a function of $[HCO_3^-]$ (0–1 mM).

in the HCO_3^- concentration range 0–1 mM. Above $[HCO_3^-] = 1$ mM, the reaction rate appears to be independent of reaction (6). Hence, the HCO_3^- concentration independent rate constant of approximately 4.4×10^{-6} m min^{-1} (mean value) should be the true rate constant for oxidation of UO_2 by H_2O_2. The HCO_3^- concentration independence also implies a negligibly low steady-state concentration of oxidized UO_2 on the particle surface ($(UO_2)_{n-1}UO_{2(s)}^{2+}$). This can be expressed as:

$$\frac{d[(UO_2)_{n-1}UO_{2(s)}^{2+}]}{dt} = k_5[H_2O_2][UO_2] - k_6[(UO_2)_{n-1}UO_{2(s)}^{2+}] \times [HCO_3^-]^x = 0 \quad (7)$$

where x is the reaction order with respect to HCO_3^-. Judging from Fig. 4, the reaction is first order with respect to HCO_3^- (the observed rate constant increases linearly with $[HCO_3^-]$) and hence $x = 1$.

The rate constant k_6 is then given by:

$$k_6 = \frac{k_5[H_2O_2][UO_2]}{[(UO_2)_{n-1}UO_{2(s)}^{2+}][HCO_3^-]} \quad (8)$$

If we assume the steady-state concentration of oxidized UO_2 on the particle surface $(UO_2)_{n-1}UO_{2(s)}^{2+}$ to be less than 1% of the total surface we obtain $k_6 \geqslant 8.8 \times 10^{-3}$ m min^{-1}. Although expressing the rate constant on the basis of the surface to volume ratio is very questionable in this case, the result implies that the rate constant for HCO_3^- facilitated dissolution of oxidized UO_2 is essentially diffusion controlled. The diffusion controlled rate constant for this system is approximately 10^{-3} m min^{-1} [7].

As previously mentioned, the zeroth order behaviour observed in experiments where $[HCO_3^-]$ is low can be attributed to a change in the rate determining step from oxidation to dissolution (not facilitated by HCO_3^-). In Table 2, the zeroth order rates and the approximate H_2O_2 conversions (hereafter denoted critical conversion) at which the reaction order changes from 1 to 0 are presented for two experimental series.

As expected, the H_2O_2 conversion at which the reaction order changes is lower for the lowest HCO_3^- concentration (0 mM added HCO_3^-). The critical H_2O_2 conversion increases with increasing amount of UO_2 and closer inspection of the results reveals an almost constant ratio between the critical conversion and the amount of UO_2 in the experi-

Table 2
Zeroth order rates and approximate H_2O_2 conversions (critical conversion) at which the reaction order changes from 1 to 0 for $[HCO_3^-] = 0$ mM and $[HCO_3^-] = 0.1$ mM

m(UO_2)/mg	$[HCO_3^-] = 0$ mM		$[HCO_3^-] = 0.1$ mM	
	H_2O_2 conversion	Rate/M min^{-1}	H_2O_2 conversion	Rate/M min^{-1}
50	0.20	4.4×10^{-5}	0.28	9.6×10^{-5}
75	0.31	1.1×10^{-4}	0.45	9.1×10^{-5}
100	0.38	1.4×10^{-4}	0.53	1.2×10^{-4}
150	0.57	1.9×10^{-4}	0.66	1.3×10^{-4}

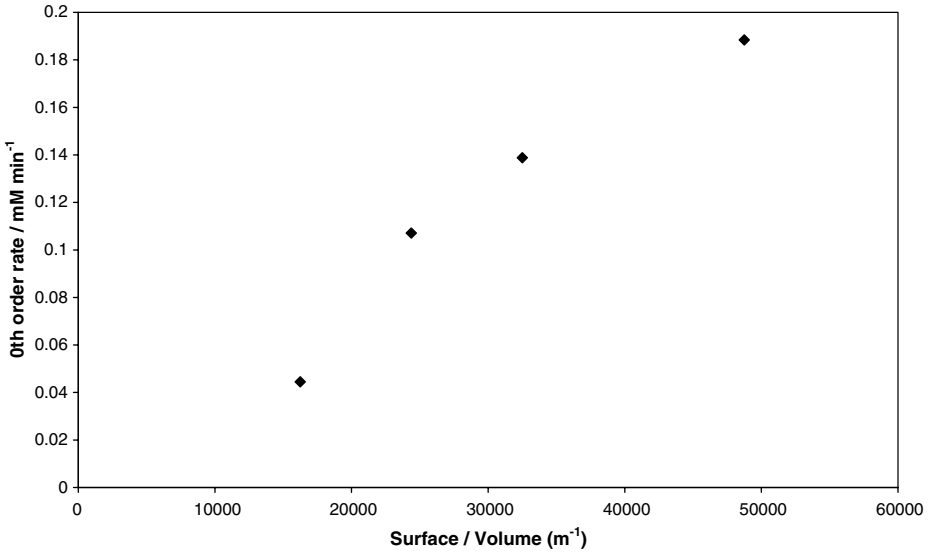

Fig. 5. Zeroth order rate for oxidation of UO_2 by H_2O_2 ($[HCO_3^-] = 0$) plotted against the surface area to solution volume ratio.

mental series where no HCO_3^- was added. In the experimental set ups used in this work, the concentration of H_2O_2 is reduced by 0.07 mM per mg UO_2 powder when the critical H_2O_2 conversion is reached. As the change in reaction order implies that the surface is saturated, the reduction in H_2O_2 concentration at the critical H_2O_2 conversion can be used to estimate the oxidation site density on the UO_2 powder used. In this particular case the estimated oxidation site density is 2.1×10^{-4} mol m^{-2} corresponding to 126 sites nm^{-2}. This is somewhat lower than the value reported by Clarens et al. (165 ± 10 sites nm^{-2}) [18] based on acidic site density. It should, however, be noted that these two values were determined using completely different methods on UO_2 powders with different specific surface areas. In view of this, the values are surprisingly similar.

As can be seen in Table 2, the zeroth order rate also depends on the amount of UO_2, i.e. on the surface area to solution volume ratio. This is particularly evident for the series where no HCO_3^- was added to the solution. In Fig. 5 the zeroth order rate is plotted against the surface area to volume ratio.

The dependence is close to linear and from the slope we can obtain the first order (with respect to UO_2 surface area to solution volume ratio) rate constant for dissolution of UO_2^{2+} from the oxidized surface. The resulting rate constant is $4.2 \pm 0.7 \times 10^{-9}$ mol dm^{-3} m min^{-1} ($7 \pm 1 \times 10^{-8}$ mol m^{-2} s^{-1}). Interestingly, this rate constant is significantly (more than one order of magnitude) higher than previously reported rate constants for UO_2 dissolution in the presence of H_2O_2 [11,19]. It should be noted that the previously reported values are based on measurements of uranium release while our value is based on consumption of H_2O_2. As the previously reported dissolution rates have been shown to depend on the H_2O_2 concentration in the system one must conclude that the UO_2-surfaces were not fully oxidized. Hence, the oxidized surface area exposed to the solution was smaller than the total UO_2 surface area (on which the dissolution rates are based). In our case, we determine the dissolution rate in a system where there is no dependence on the H_2O_2 concentration (zeroth order kinetics) and consequently the surface is expected to be fully oxidized.

In conclusion, the rate constants for oxidation of UO_2 by H_2O_2, HCO_3^- facilitated dissolution of UO_2^{2+} and dissolution of UO_2^{2+} in pure water are given in Table 3.

Table 3
Rate constants for oxidation of UO_2 by H_2O_2, HCO_3^- facilitated dissolution of UO_2^{2+} and dissolution of UO_2^{2+} in pure water

Reaction	Rate constant
$H_2O_2 + UO_{2(s)} \rightarrow 2OH^- + UO_{2(s)}^{2+}$	4.4×10^{-6} m min^{-1}
$HCO_3^- + UO_{2(s)}^{2+} \rightarrow UO_2CO_{3(aq)} + H^+$	$\geqslant 8.8 \times 10^{-3}$ m min^{-1}
$UO_{2(s)}^{2+} \rightarrow UO_{2(aq)}^{2+}$	$7 \pm 1 \times 10^{-8}$ mol m^{-2} s^{-1}

Acknowledgement

SKB is gratefully acknowledged for financial support.

References

[1] D.W. Shoesmith, J. Nucl. Mater. 282 (2000) 1.
[2] R.L. Segall, R.S.C. Smart, P.S. Turner, Oxide Surfaces in Solution, in: L.-C. Dufour (Ed.), Surface and Near-Surface Chemistry of Oxide Materials, Elsevier Science Publishers B.V., Amsterdam, 1988, p. 527.
[3] J.W.T. Spinks, R.J. Woods, An Introduction to Radiation Chemistry, John Wiley and Sons Inc., New York, 1964.
[4] P. Wardman, J. Phys. Chem. Ref. Data 18 (1989) 1637.
[5] R.E. Huie, C.L. Clifton, P. Neta, Rad. Phys. Chem. 38 (1991) 477.
[6] I. Grenthe, F. Diego, F. Salvatore, G. Riccio, J. Chem. Soc. Dalton Trans. 11 (1984) 2439.
[7] E. Ekeroth, M. Jonsson, J. Nucl. Mater. 322 (2003) 242.
[8] P.W. Atkins, Physical Chemistry, fifth ed., Oxford University Press, Oxford, 1994, Ch. 24.
[9] J.B. Hiskey, Miner. Process. Extractive Metall. 89 (1980) C145.
[10] K.C. Liddell, R.G. Bautista, Metall. Mater. Trans. B: Proc. Metall. Mater. Process. Sci. 26B (1995) 695.
[11] J. de Pablo, I. Casas, F. Clarens, F. El Aamrani, M. Rovira, Mater. Res. Soc. Symp. Proc. 663 (2001) 409.
[12] J. Bruno, E. Cera, T.E. Eriksen, M. Grivé, S. Ripoll, Mater. Res. Soc. Symp. Proc. 807 (2004) 397.
[13] D.E. Richardson, H. Yao, K.M. Frank, D.A. Bennett, J. Am. Chem. Soc. 122 (2000) 1729.
[14] A.B. Ross, B.H.J. Bielski, G.V. Buxton, D.E. Cabelli, C.L. Greenstock, W.P. Helman, R.E. Huie, J. Grodkowski, P. Neta, NDRL/NIST Solution Kinetics Database, 1992.
[15] W.A. Patrick, H.B. Wagner, Anal. Chem. 21 (1949) 1279.
[16] T.C.J. Ovenston, W.T. Rees, Analyst 75 (1950) 204.
[17] Y. Nimura, K. Itagaki, K. Nanba, Nippon Suisan Gakkaishi 58 (1992) 1129.
[18] F. Clarens, J. de Pablo, I. Casas, M. Giménez, M. Rovira, Mater. Res. Soc. Symp. Proc. 807 (2004) 71.
[19] F. Clarens, J. de Pablo, I. Casas, J. Giménez, M. Rovira, J. Merino, E. Cera, J. Bruno, J. Quinones, A. Martinez-Esparza, J. Nucl. Mater. 345 (2005) 225.